KAMPALA INTERNATIONAL UNIVERSITY
EXPLORING THE HEIGHTS

KIU
Journal of Science, Engineering and Technology

KJSET Research Article

Simulation study on Benfield's hot potassium carbonate electrolyte system: Effects of temperature, pressure, and concentration on solubility index

Omer Eisa Babiker [1] & Omar Suliman Zaroog[2]
Department of Mechanical Engineering, Kampala International University, Uganda [1,2]
omar.eisa@kiu.ac.ug [1], omar.zaroog@kiu.ac.ug[2]

Corresponding Author: omar.eisa@kiu.ac.ug

Paper history:
Received 29 December 2024
Accepted in revised form 14 March 2025

Keywords
Benfield system; electrolyte, solution; crystallization; solubility index.

Abstract

Benfield's Electrolyte system known as potassium carbonate aqueous solution has been analyzed to investigate the solubility index in varying temperatures, pressures, and concentrations. Redlich-Kwong thermodynamic model has been used to calculate the vapor-liquid equilibrium between water and carbon dioxide. In contrast, the electrolyte non-random two-liquid (ELECNRTL) model is used to model the activity coefficient, transport properties, and solubility index. The model extended for the system of carbonate/bicarbonate mixture at a temperature range of 280- 403 K, pressure of 1 and 2 bar, and carbonate/bicarbonate concentrations ranging between 2.1706/0.0 and 0.0/2.9954 mole/kg H_2O. A case study was performed on the crystallization of electrolytes K_2CO_3 and $KHCO_3$ in the Benfield process to demonstrate the model applications. The results suggest the possibility of operations error that may have initiated salt crystallization through excessive heating or draining of the HPC solution. The outcome results showed a large deviation from the normal tendency for the transport properties and solubility index at an approximate temperature of 377 K. The simulation results showed a sufficient accuracy for the 30 wt% HPC solution with errors between the simulation results and the published data within 1 to 5%.

1.0 Introduction

The Benfield process, developed by Benson et al. [1] In the mid-1950s, was an important commercial technology for removing acid gas from natural gas streams. The Benfield process is based on the method of chemical absorption, in which a solution of hot potassium carbonate (HPC) reacts with an acid gas, for example, carbon dioxide (CO_2), to form carbonate and bicarbonate. Figure 1 shows a typical Benfield process flow scheme comprising an absorber and a regenerator. Natural gas streams carrying acid gases contact counter-currently with a lean HPC solution in the Benfield absorber. The treated natural gas exits the top of the Benfield absorber at low temperature. It normally contains less than 50 ppm CO_2 and 1 ppm H_2S by volume [1]. The rich HPC solution exiting from the bottom of the Benfield absorber is stripped in the regenerator at elevated temperature and liberates the acid gases. Two reboilers heat the condensate and bottom streams before returning them to the bottom of the Benfield regenerator. The lean HPC solution exits the bottom of the Benfield regenerator and is recycled to the absorber. The HPC solution normally contains 20 wt% or 40 wt% K_2CO_3 solvent, 1-3 wt% di-ethanol amine activator, 0.4 wt% and 0.7 wt% vanadium pentoxide as corrosion inhibitor, and the balance is water. The absorption of CO_2 is normally performed at a temperature range of 70 to 140oC and pressure between 1 and 2 bar [1]. The Benfield process has several unique advantages over other acid gas removal systems including a larger capture CO_2 capacity to even in the existence of other different components such as Sulphur-dioxide, operations at a higher temperature making the separation more efficient, low cost, low toxicity, and low degradability [2–5]. On the other hand, the HPC solution may generate salt crystals inside the system that leads to fouling. The fouling problem is especially critical in the heat exchangers and the lean solution transporting pipes around the reboilers of the Benfield regenerator unit [6,7]. Hence, an analysis of salt formation in the HPC solution is essential to gain insights into effective operating windows to avoid the fouling problem. The analysis is applied to the thermodynamics of the electrolyte system [8]. The effects of changing operating conditions such as temperature, pressure, and solute concentrations on the transport properties of HPC solutions. Numerous studies have been performed on process modification in terms of solvent concentrations, process conditions, and process design. The modifications conducted in seven altered process setups have been examined to assess their effects on the performance of a standard K_2CO_3 capture system [9]. The alteration of the rich solvent pre-heating and the compression of the lean vapor were found to reduce the specific stripper reboiler duty by 24.28% and 21.38%, respectively. In the current simulation study, following properties were examined: heat capacity, activity coefficient, saturation index, viscosity to investigate the variation of the solvent solution density.

2.0 Solution and Electrolyte Reactions

The HPC solution's chemical composition is identified by ionic species produced by water dissociation and solid hydration reactions. The details of the equilibrium reaction for the absorption of CO_2 in aqueous carbonate solution consist of seven reaction components [10,11,12,13] as explained below.

$$K_2CO_3 \leftrightarrow 2K^+ + CO_3^{2-} \quad (1)$$

$$KHCO_3 \leftrightarrow K^+ + HCO_3^- \quad (2)$$

Reactions (1) and (2) are defined as the dissociation of K2CO3 and $KHCO_3$ in H_2O to generate (K^+), (CO_3^{2-}) and (K^+), ($HCO3^-$) ions. Hydrolysis and ionization of dissolved CO_2 to (H_3O^+) and bicarbonate ions (HCO_3^-) is described by reaction (3).

$$CO_2 + 2H_2O \leftrightarrow HO^- + HCO_3^- \quad (3)$$

Reaction (4) designates the ionization of (HCO3-) to (H_3O^+) and (CO_3^{2-}) while equation (5) for water dissociations to (H_3O^+) and (OH-) ions.

$$HCO_3^- + H_2O \leftrightarrow H_3O^+ + CO_3^{2-} \quad (4)$$

$$2H_2O \leftrightarrow HO_3^+ + OH^- \quad (5)$$

Salt dissociation reactions of carbonate and bicarbonate are described by reactions (6) and (7).

$$K_2CO_{3(S)} \leftrightarrow 2K^+ + CO_3^{2-} \quad (6)$$

$$KHCO_{3(S)} \leftrightarrow K^+ + HCO_3^- \quad (7)$$

Reactions (1) to (7) together provide the overall chemical absorption equilibrium reaction as shown below:

$$K_2CO_3 + CO_2 + H_2O \leftrightarrow 2KHCO_3 \quad (8)$$

3.0 Modelling and Simulation

Aspen Plus simulator V.12.4 along with the Aspen database [14] is used for modeling the electrolyte systems of HPC solution. Aqueous electrolyte K_2CO_3 thermodynamics and physical properties in the vapor-liquid phase equilibrium are calculated using two models. Water and carbon dioxide vapor-liquid equilibrium is modeled using the Redlich-Kwong EOS model, whereas the activity coefficient is modeled using the electrolyte non-random two-liquid (ELECNRTL) model.

[10, 12, 14]. The ELECNRTL model is available in Aspen Plus with built-in property estimation packages. Figure 2 shows the algorithm for simulating the Benfield Process electrolyte system. The ELECNRTL model is more appropriate than other models, such as the Pitzer model. This is because the ELECNRTL model includes the temperature dependence of ion interaction parameters. Furthermore, the model can estimate the properties of aqueous solutions even at medium and high concentrations [15].

The ionic force between the different ionic species forms a framework for the thermodynamic computation of the electrolyte system utilizing the ELECNRTL model. The number and kind of species, as well as the distance between them, all affect the ionic force.

The energy parameters (GMELCC, GMELCD, and GMELCE) and non-randomness factors (GMELCN) for several molecule-electrolyte and electrolyte-electrolyte combinations are available in the ELECNRTL databank in Aspen Plus. The dielectric constant ε_B of solvent molecule B is defined as a function of temperature T by a general polynomial relation,

$$\varepsilon_B(T) = A_B + B_B\left(\frac{1}{T} - \frac{1}{C_B}\right)$$

Where; A, B, and C are fitting coefficients. In addition, the temperature dependency relations of electrolyte NRTL for molecule-molecule binary parameters are shown in equation (10).

$$\tau_{BB'} = A_{BB'} + \frac{B_{BB'}}{T} + F_{BB'}\ln(T) + G_{BB'}T$$

In equation (11), τ is the electrolyte NRTL energy parameter. For systems of pair parameters, the temperature dependency relations are given in equations (12) and (13) for the electrolyte-molecule pair and in equations (14) and (15) for the electrolyte-electrolyte pair, respectively.

$$\tau_{ca,B} = C_{ca,B} + \frac{D_{ca,B}}{T} + E_{ca,B'}\left[\frac{\left(T^{ref} - T\right)}{T} + \ln\left(\frac{T}{T^{ref}}\right)\right] \quad (11)$$

$$\tau_{B,ca} = C_{B,ca} + \frac{D_{B,ca}}{T} + E_{B,ca}\left[\frac{\left(T^{ref} - T\right)}{T} + \ln\left(\frac{T}{T^{ref}}\right)\right] \quad (12)$$

$$\tau_{c'a,c''a} = C_{c'a,c''a} + \frac{D_{c'a,c''a}}{T} + E_{c'a,c''a}\left[\frac{\left(T^{ref} - T\right)}{T} + \ln\left(\frac{T}{T^{ref}}\right)\right] \quad (13)$$

$$\tau_{ca',ca''} = C_{ca',ca''} + \frac{D_{ca',ca''}}{T} + E_{ca',ca''}\left[\frac{\left(T^{ref} - T\right)}{T} + \ln\left(\frac{T}{T^{ref}}\right)\right] \quad (14)$$

Table 1 shows the electrolyte pair energy parameters C, D, and E used in the governing equations above for the temperature dependency equations [14]. The reference temperature Tref is at 298.15 K.

A variable model for determining the activity coefficient is ELECNRTL. Both a mixed solvent and an aqueous electrolyte system can be represented by the model using binary and pair parameters. The activity coefficient and mean activity coefficient ($\gamma\pm$) for molecular and ionized species in an aqueous electrolyte system are also computed using the following relation [16].

$$\gamma\pm = \left(\gamma_+^{\,x}\gamma_-^{\,y}\right)^{\frac{1}{(x+y)}} \quad (15)$$

where x, and y are the number of cations and anions, respectively. The following expression is a description of the activity coefficient equation for molecular components [14]:

$$\ln\gamma_B^{\,lc} = \frac{\sum_j X_j G_{jB}\tau_{jB}}{\sum_k X_k G_{kB}} + \sum_{B'}\left(\frac{X_{B'}G_{BB'}}{\sum_k X_k G_{kB'}}\right)\left(\tau_{BB'} - \frac{\sum_k X_k G_{kB'}\tau_{kB'}}{\sum_k X_k G_{kB'}}\right) + \sum_c\sum_{a'}\frac{X_a}{\sum_{a''}X_{a''}}\frac{X_c G_{Bc,a'c}}{\sum_k X_k G_{kc,a'c'}}\left(\tau_{Bc,a'c} - \frac{\sum_k X_k G_{kc,a'c}\tau_{kc,a'c}}{\sum_k X_k G_{kc,a'c}}\right) + \sum_c\sum_{a'}\frac{X_{c'}}{\sum_{c''}X_{c''}}\frac{X_a G_{Ba,c'a}}{\sum_k X_k G_{ka,c'a}}\left(\tau_{Bc,c'a} - \frac{\sum_k X_k G_{ka,c'a}\tau_{ka,c'a}}{\sum_k X_k G_{ka,c'a}}\right) \quad (16)$$

Equation (17), presents the activity coefficient relation for cations.

$$\frac{1}{z_c}\ln\gamma_c^{\,lc} = \sum_{a''}\frac{X_{a'}}{\sum_{a''}X_{a''}}\frac{\sum_k X_k G_{kc,a'c}\tau_{kc,a'c}}{\sum_k X_k G_{kc',a'c'}} + \sum_{B'}\left(\frac{X_B G_{cB}}{\sum_k X_k G_{kB}}\right)\left(\tau_{cB} - \frac{\sum_k X_k G_{kB}\tau_{kB}}{\sum_k X_k G_{kB}}\right) + \sum_a\sum_{c'}\frac{X_{c'}}{\sum_{c''}X_{c''}}\frac{X_c G_{ca,a'c}}{\sum_k X_k G_{ka',c'a}}\left(\tau_{ca,c'a} - \frac{\sum_k X_k G_{ka,c'a}\tau_{ka,c'a}}{\sum_k X_k G_{ka,c'a}}\right) \quad (17)$$

while for anions is given by equation (18).

$$\frac{1}{z_a}\ln\gamma_a^{\,lc} = \sum_{c'}\frac{X_{c'}}{\sum_{c''}X_{c''}}\frac{\sum_k X_k G_{ka,c'a}\tau_{ka,c'a}}{\sum_k X_k G_{ka',c'a}} + \sum_B\left(\frac{X_B G_{cB}}{\sum_k X_k G_{kB}}\right)\left(\tau_{cB} - \frac{\sum_k X_k G_{kB}\tau_{kB}}{\sum_k X_k G_{kB}}\right) + \sum_a\sum_{c'}\frac{X_{c'}}{\sum_{c''}X_{c''}}\frac{X_c G_{ca,a'c}}{\sum_k X_k G_{ka',c'a}}\left(\tau_{ca,c'a} - \frac{\sum_k X_k G_{ka,c'a}\tau_{ka,c'a}}{\sum_k X_k G_{ka,c'a}}\right) \quad (18)$$

An important thermodynamic property for the analysis of crystallization is the Solubility Index (SI). In electrolyte systems such as HPC solutions, if the SI of the salt is bigger than 1, then the compound is present as a solid. Conversely, a saturation index (SI) value less than 1 signifies that the salt has not attained saturation and will remain in the aqueous solution. The solubility index is characterized as the proportion of the activity product of the salt to the solubility product [8, 17],

$$SI = \frac{\prod_{i=1}^{NC} a_i^{\,v_{ij}}}{K_j} = \frac{a_k^{\,k}\,a_A^{\,\infty}\,a_w^{\,n}}{K_{k_k}\,A_a H_2O} \quad (19)$$

Where:

$$K = e^{\left(-\frac{\Delta G^0}{RT}\right)} = e^{\left(\sum \ln a_i v_i\right)} \quad (20)$$

4.0 Results and Discussions

The thermodynamic evaluation of the Benfield process focuses on a 30 wt% HPC solution, and the mixture of carbonate and bicarbonate has been discussed by O. Eisa and M. Shuhaimi [19]. The transport characteristics of HPC solution, including viscosity, density, and saturation index, are evaluated for a temperature span from the freezing point to the boiling point, specifically from 283.15 K to 366.15 K. The study continued in this work to examine the performance of carbonate/bicarbonate concentration

ratios on the liquid density, solution activity coefficient, and solubility index at 1 and 2 bar pressures.

4.1 Model Validation

The simulation results for HPC solution viscosity between 280.15 K and 370.15 K, O Eisa, and M Shuhaimi [19] are associated with the data presented by Kohl and Nielsen [1]. The viscosity of the HPC solution is higher at lower temperatures and shows a decreasing trend until it reaches the boiling temperature. Beyond the boiling point, the viscosity simulations start to deviate from the experimental measurements. The divergence may be attributed to the evaporation of water that affects the solvent volume in the viscosity calculations. However, the predicted boiling temperature of 362.15 K from the simulation results acceptably agrees with the reported value [1] with an error of -1.1%. The solubility index of HPC solutions was calculated in the temperature range of 280 K to 370 K [19]. At the saturation point of SI=1, the predicted freezing point is 287 K, which decides well with the data that described by Kohl and Nielsen [1] with a (+1.4 %) error. In addition, the profile of the simulated HPC solution density. From the density results, the calculated specific gravity (SG) values have been reported by O Eisa, and M Shuhaimi [19] and compared with the reported experimental SG values [1]. The comparison showed excellent results with an average error of less than 1.5%. The estimated profile of the activity coefficient showed a clear increase with the increases in operating temperature and it showed an acceptable agreement with the literature values [19] and it has an average error of less than 5%. The high degree of agreement between all the simulated transport properties [19] and the published values in the literature strengthens the validity of the model used in this study. Consequently, the study is further extended to examine the effect of operating parameters on the crystal formation in a solution containing a mixture of carbonate/bicarbonate solution. The carbonate/bicarbonate mixture reflects the actual solution that exists in the reboilers of a Benfield process regenerator unit.

4.2 Case Study: Crystallization in reboilers at a Benfield process regenerator unit

This case study concerns a crystallization problem at the reboilers of a Benfield process regenerator unit in a fertilizer plant. The Benfield process includes two reboiler units designed with a shell and tube configuration, featuring two passes for the tubes. Following a scheduled inspection of the tube bundle, an aqueous carbonate solution was discharged from the reboiler bottom drain valves after the system was shut down. The first reboiler was completely drained. Upon conducting an internal examination, several areas on the shell side were discovered to have a black solid coating. Moreover, the draining process of the second reboiler was not fully completed, and an inspection revealed that approximately 60% of the unit was submerged in a crystallized solution. The tube bundle was unable to be extracted for inspection.

The simulation of an aqueous solution containing a carbonate/bicarbonate mixture is carried out by considering different carbonate/bicarbonate concentration ratios. The initial carbonate (K_2CO_3) concentration is 2.17 mole/Kg H_2O. It is presumed that the complete conversion of carbonate to bicarbonate ($KHCO_3$) occurs during the absorption phase and that all bicarbonate reverts to carbonate during the regeneration phase, as outlined in reaction (8). These assumptions are essential for assessing the characteristics of mixed carbonate/bicarbonate solutions under different pressures and temperatures. The current analysis was conducted for various concentration ratios over a temperature range of 298 to 403 K and at pressures between 1 and 2 bars. As shown in Table 1, the initial ratio of 2.1706/0.0 carbonate/bicarbonate for 30 wt% HPC solution is for zero conversion. Furthermore, for 100% conversion, the ratio of carbonate/bicarbonate is 0.0/2.9953.

Figure-3 shows the results of the carbonate/bicarbonate mixture solution density as a function of the concentration. The densities of the simulated solutions increase with elevated carbonate concentrations and decrease with higher bicarbonate concentrations. For a mixture ratio of 2.1706/0.0, the solution density declines as the temperature rises until reaching the boiling point of 378 K at 1 bar pressure and 396 K at 2 bar. For various mixture ratios between 1.9294/0.3328 and 0.0/2.9954, the density exhibits a different trend due to the presence of the bicarbonate anion (HCO3-). The density increases with temperature from 298 K to around 312 K at 1 bar and 322 K at 2 bar before it decreases beyond these points until its boiling temperatures. The density increase is observed at low temperatures when the activity coefficient of the bicarbonate anions is usually higher than unity. Beyond the boiling points, carbonate/bicarbonate solution densities increase rapidly for all concentration ratios due to the sudden change of liquid volume.

The simulated water activity coefficient at varying temperatures and pressures for the aqueous carbonate/bicarbonate mixture solution is shown in Figure 4. As the carbonate concentration reduces from 2.1706 to 0.0 mole/Kg H_2O, the water activity coefficient increases for both system pressures at 1 bar and 2 bar raising the temperature from 298 K to 378 K enhances the water activity coefficient as a result of water dissociation and the solubility of the carbonate/bicarbonate mixture. However, beyond 378.15 K, water activity coefficients decrease rapidly for the entire aqueous carbonate/bicarbonate mixture solution. This is likely a result of the impact that boiling has on the volume of the liquid.

The solubility index of the carbonate/bicarbonate mixture solution is found to decrease with increasing bicarbonate concentrations. The solubility index reduces with rising temperatures until it reaches the boiling point of the solution. Once surpassing the boiling point, the solubility index begins to increase significantly

once more. The solubility index profiles to the carbonate/bicarbonate ratio and temperature at pressures of 1 and 2 bars are illustrated in Figure 5 and Figure 6, respectively. In this study, the solubility index is observed to be lower than unity for all carbonate/bicarbonate mixture solutions at temperatures lower than 396 K and at 1 bar as observed in Figure 5. Figure 6 shows a similar observation for the solubility index of bicarbonate at different ratios of carbonate/bicarbonate mixture solutions. The results from these simulations suggest that fouling could not have occurred due to process design errors. However, it is interesting to observe that for both cases of pressure at 1 and 2 bar in Figures 9 and 10, sufficiently high temperature may push the solubility index rapidly to above unity. In other words, excessive heating may initiate the formation of salt crystals that eventually lead to fouling of the reboilers in the Benfield process regenerator unit. Moreover, excessive draining of HPC solution by process operators to replace it with a new solution may also leave behind a high concentration of bicarbonate for approximately a duration of time. As shown in Figure 6, a high concentration of bicarbonate component is more likely to cause crystals at the given critical conditions. It is commonly noted that functioning at a pressure of 2 bar allows for a broader variety of liquid phases, thereby diminishing the likelihood of crystallization. Tables (2) and (3) display the simulation outcomes for water activity, viscosity, density, and solubility index at the minimum, medium, and maximum temperatures of 298, 344, and 403 K, respectively, under pressures of 1 bar and 2 bar.

5.0 Conclusions

The simulation of HPC solvent in the Benfield process using the ELECNRTL model has generated some interesting results. These results provide insights into the operating parameters to avoid crystallization problems. A series of simulations have been performed to investigate the relationships between the system's temperature, pressure as well as concentrations of solvent on the viscosity, activity coefficient, density, and solubility index of HPC solutions. The model underwent validation against published data and demonstrated an accuracy level within an error margin of 1 to 5%. The simulation was conducted for high-performance computing solutions that included 30 wt% potassium carbonates, consisting of a mix of carbonate and bicarbonate. The 30 wt% potassium carbonate solution was modeled at temperatures varying from 280 K to 370 K and pressures of 1 and 2 bar, while the carbonate/bicarbonate mixture was modeled at temperatures from 280 to 403 K, under pressures of 1 and 2 bar, with carbonate/bicarbonate concentrations ranging from 2.1706/0.0 to 0.0/2.9954 mole/kg H_2O. The effects of changing operating conditions showed that the boiling point of HPC solutions has a significant impact on the transport properties. At this point, the density and solubility index increase rapidly and the water activity coefficient reduces rapidly. Based on the simulation results, it was proposed that excessive heating of reboilers in the Benfield process regenerator unit may have caused a rapid rise of the saturation index of the carbonate/bicarbonate solutions and initiated the formation of salt crystals that eventually lead to fouling of the reboilers.

Acknowledgment

Petronas Gas Company acknowledged for the financial support to complete the project. Kind permission by Universiti Teknologi Malaysia to perform part of this work at the Faculty of Chemical Engineering is also duly acknowledged. Also, the authors would like to express their gratitude to the Kampala International University (KIU), Uganda

Table 1. Carbonate/bicarbonate mixture concentration

K_2CO_3/m	$KHCO_3$/m
2.1706	0.0000
1.9294	0.3328
1.6882	0.6657
1.4471	0.9985
1.2059	1.3313
0.9647	1.6641
0.7235	1.9970
0.4824	2.3298
0.2413	2.6627
0.0000	2.9953

Table 2. Results data of mixture carbonate/bicarbonate solution properties at pressure 1 bar

Concentration		Solution Property											
		γ			η / (N.sec.sqm^{-1})			ρ /(kg.cum^{-1})			*(SI)*		
m_1	m_2	*T/K*											
		298.15	343.15	403.15	298.15	343.65	403.15	298.15	343.65	403.15	298.15	343.65	403.15
2.1706	0.0000	0.7879	0.8606	0.7253	0.00483	0.00175	0.0817	1343.0	1315.6	1972.2	0.4070	0.0390	1.9210
1.9294	0.3328	0.8167	0.8757	0.7259	0.00340	0.00134	0.0596	1311.0	1303.8	1968.4	0.1540	0.0189	1.6790
1.6882	0.6657	0.8471	0.8925	0.7250	0.00244	0.00103	0.0434	1277.5	1291.4	1961.4	0.0488	0.0075	1.4489

1.4471	0.9985	0.8770	0.9088	0.7237	0.00181	0.00086	0.0352	1245.4	1279.1	1957.2	0.0133	0.0030	1.3138
1.2059	1.3313	0.9053	0.9241	0.7221	0.00141	0.00081	0.0304	1196.0	1255.0	1953.2	0.0031	0.0012	1.2290
0.9647	1.6641	0.9299	0.9380	0.7205	0.00117	0.00085	0.0273	1186.4	1243.3	1952.5	0.0006	0.0005	1.1733
0.7235	1.9970	0.9494	0.9502	0.7188	0.00112	0.00010	0.0252	1184.9	1231.6	1952.5	0.0001	0.0002	1.1352
0.4824	2.3298	0.9640	0.9602	0.7172	0.00131	0.00127	0.0236	1185.7	1220.3	1952.7	3.45E-5	8.52E-5	1.1086
0.2413	2.6627	0.9756	0.9670	0.7155	0.00187	0.00152	0.0225	1185.0	1209.6	1953.2	8.3E-06	3.8E-05	1.0906
0.0000	2.9953	0.9843	0.9713	0.7139	0.00287	0.00137	0.0217	1186.4	1243.3	1952.5	4.6E-07	2.8E-05	1.0781

Table 3. Results data of mixture carbonate/bicarbonate solution properties at pressure 2 bar

Concentration		Solution Property											
		γ			η / (N.sec.sqm^{-1})			ρ /(kg.cum^{-1})			*(SI)*		
m_1	m_2	*T/ K*											
		298.15	343.65	403.15	298.15	343.65	403.15	298.15	343.65	403.15	298.15	343.65	403.15
2.1706	0.0000	0.7879	0.8612	0.9045	0.00483	0.00173	0.00088	1342.9	1315.7	1308.9	0.4075	0.0382	0.0304
1.9294	0.3328	0.8167	0.8763	0.9059	0.00340	0.00132	0.00082	1311.1	1303.9	1313.5	0.1537	0.0186	0.0261
1.6882	0.6657	0.8471	0.8931	0.9065	0.00244	0.00102	0.00074	1277.6	1291.4	1319.0	0.0488	0.0075	0.0206
1.4471	0.9985	0.8770	0.9093	0.9053	0.00181	0.00086	0.00071	1245.4	1279.1	1325.4	0.0133	0.0030	0.0180
1.2059	1.3313	0.9053	0.9245	0.9033	0.00141	0.00080	0.00070	1216.9	1267.0	1331.7	0.0031	0.0012	0.0170
0.9647	1.6641	0.9299	0.9384	0.9010	0.00117	0.00085	0.00069	1196.1	1255.1	1337.4	0.0006	0.0005	0.0166
0.7235	1.9970	0.9494	0.9505	0.8987	0.00112	0.00099	0.00069	1186.4	1243.3	1342.5	0.0001	0.0002	0.0167
0.4824	2.3298	0.9640	0.9604	0.8965	0.00131	0.00126	0.00070	1185.0	1231.7	1347.1	3.4E-05	8.5E-05	0.0169
0.2413	2.6627	0.9756	0.9676	0.8944	0.00187	0.00169	0.00071	1185.7	1220.0	1351.2	8.3E-06	3.0E-05	0.0172
0.0000	2.9953	0.9843	0.9722	0.8925	0.00292	0.00171	0.00072	1184.6	1208.6	1355.0	2.6E-07	1.6E-05	0.0175

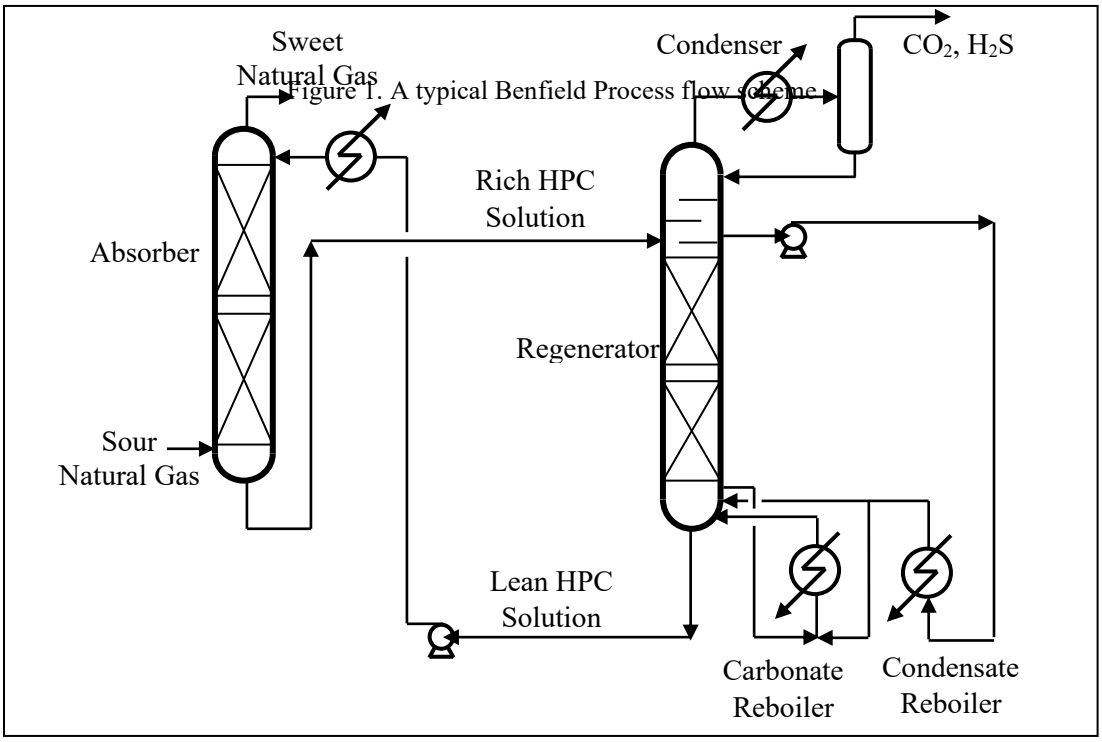

Figure 1. A typical Benfield Process flow scheme

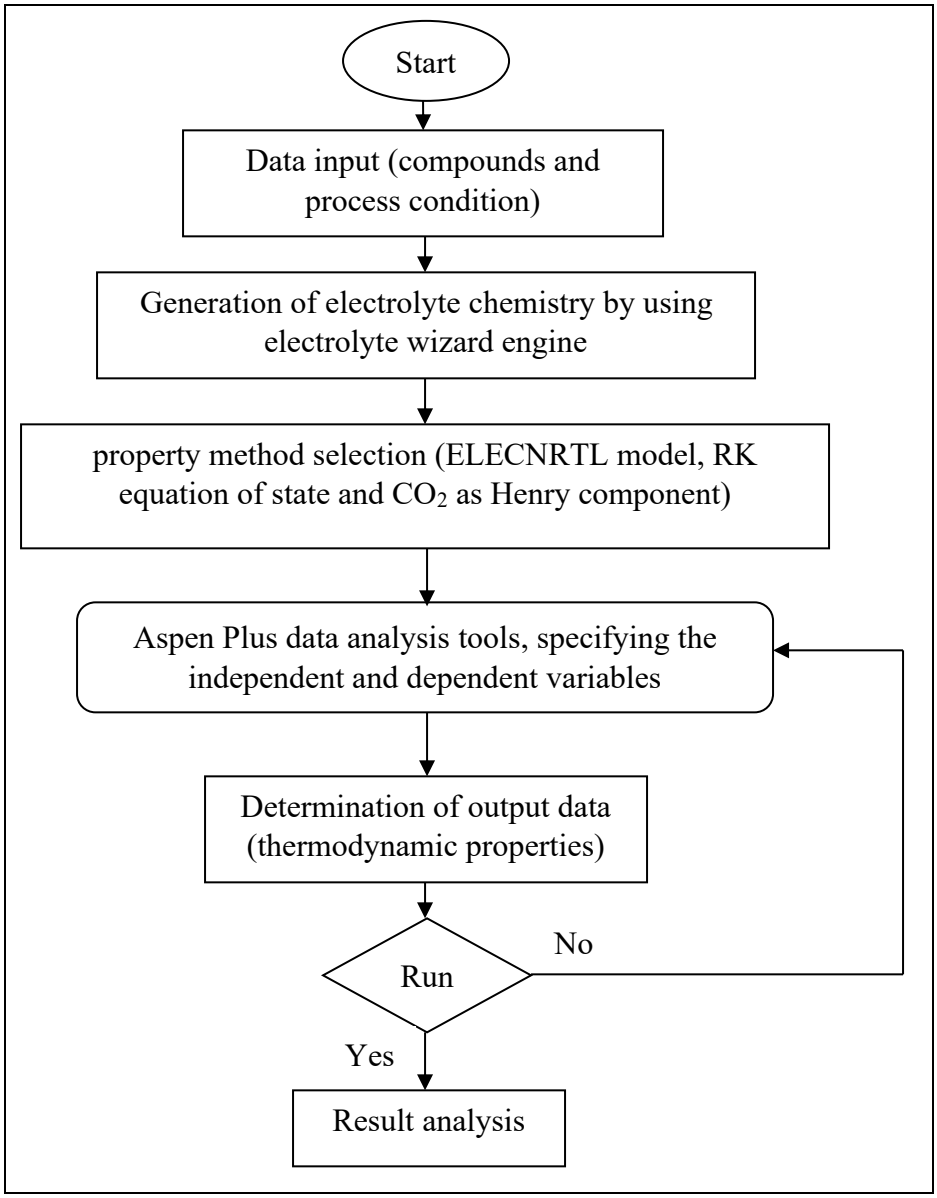

Figure 2. Electrolyte system simulation algorithm

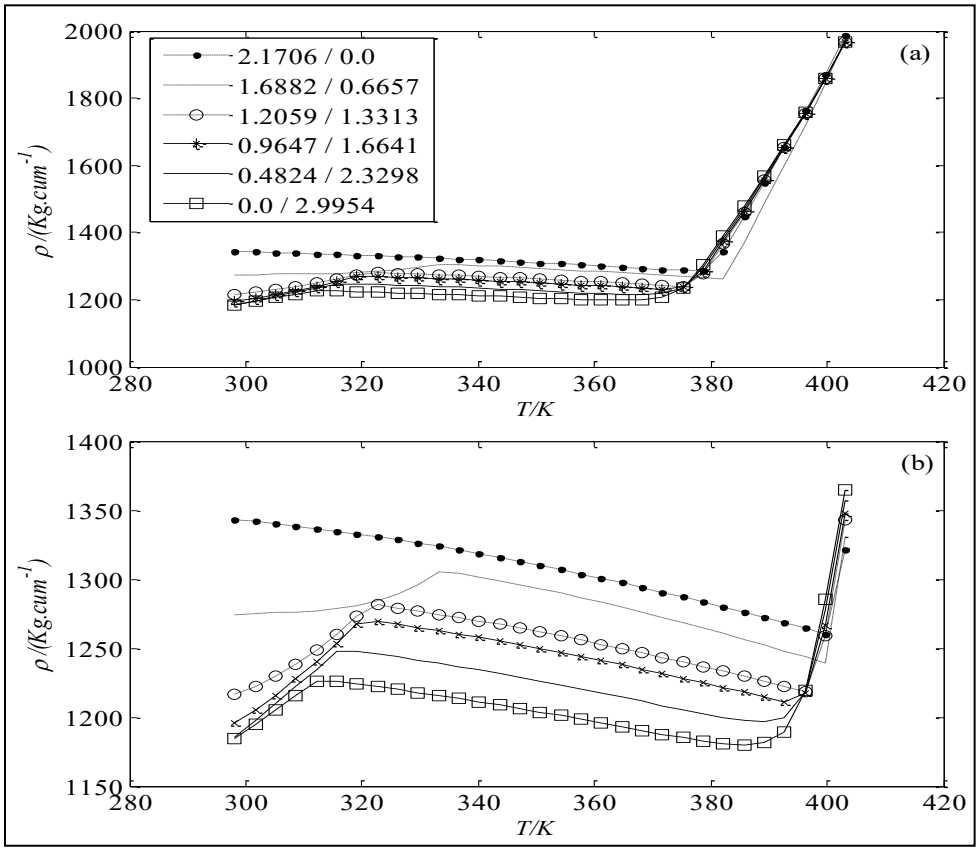

Figure 3. Effect of temperature and pressure on the liquid density for carbonate/bicarbonate mixture solution at pressures of 1 bar (a) and 2 bar (b).

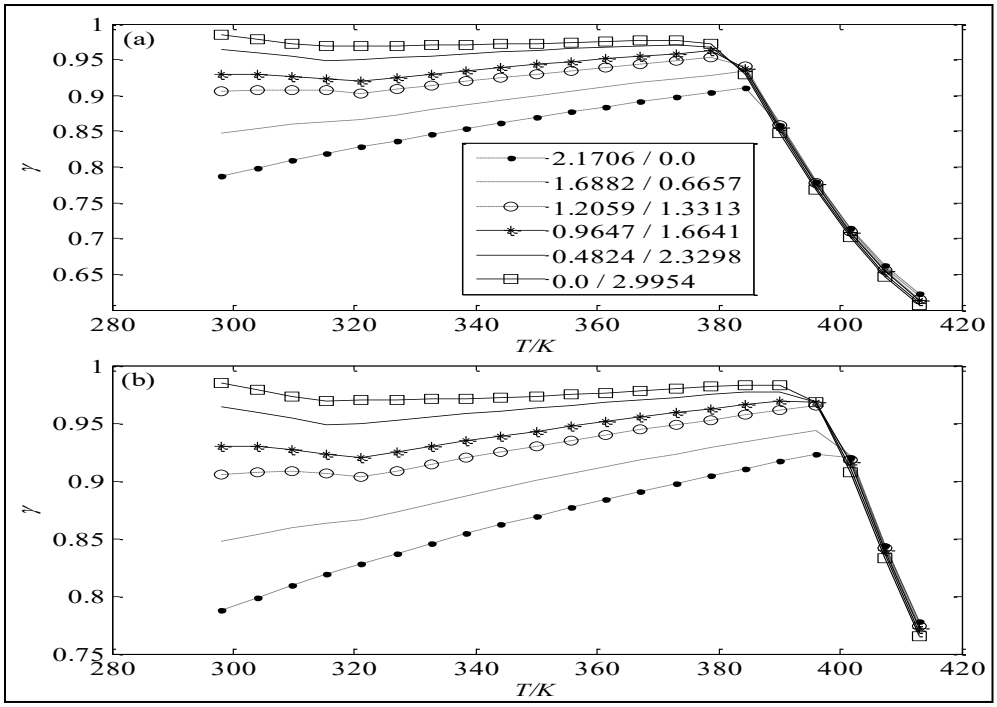

Figure 4. Effect of temperature and pressure on the water activity coefficient for carbonate/bicarbonate mixture solution at pressures of 1 bar (a) and 2 bar (b).

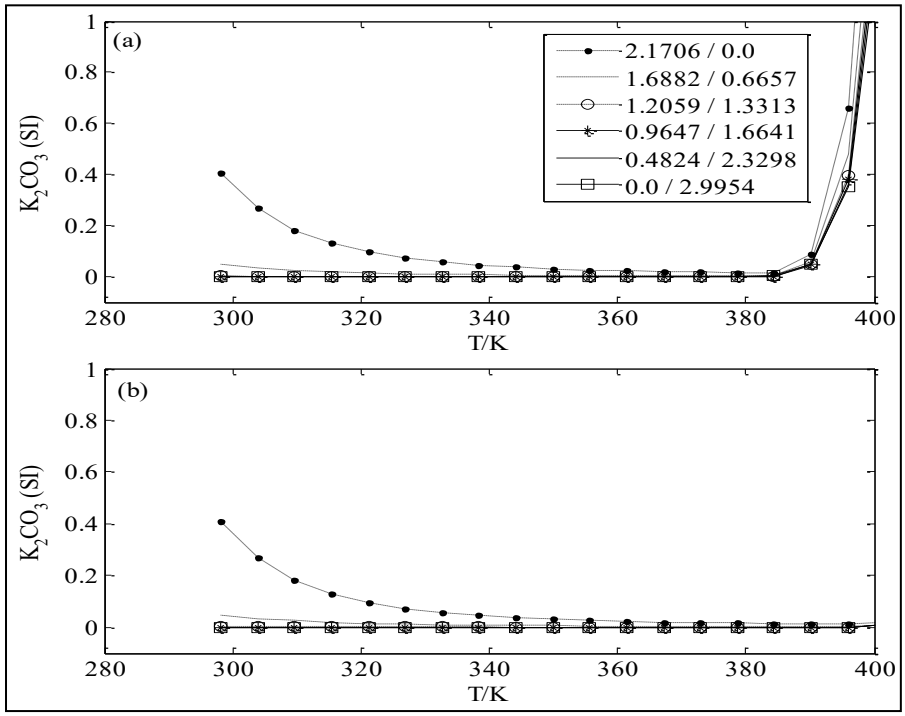

Figure 5. Effect of temperature and pressure on the K_2CO_3 solubility index for carbonate/bicarbonate mixture solution at pressures of 1 bar (a) and 2 bar (b).

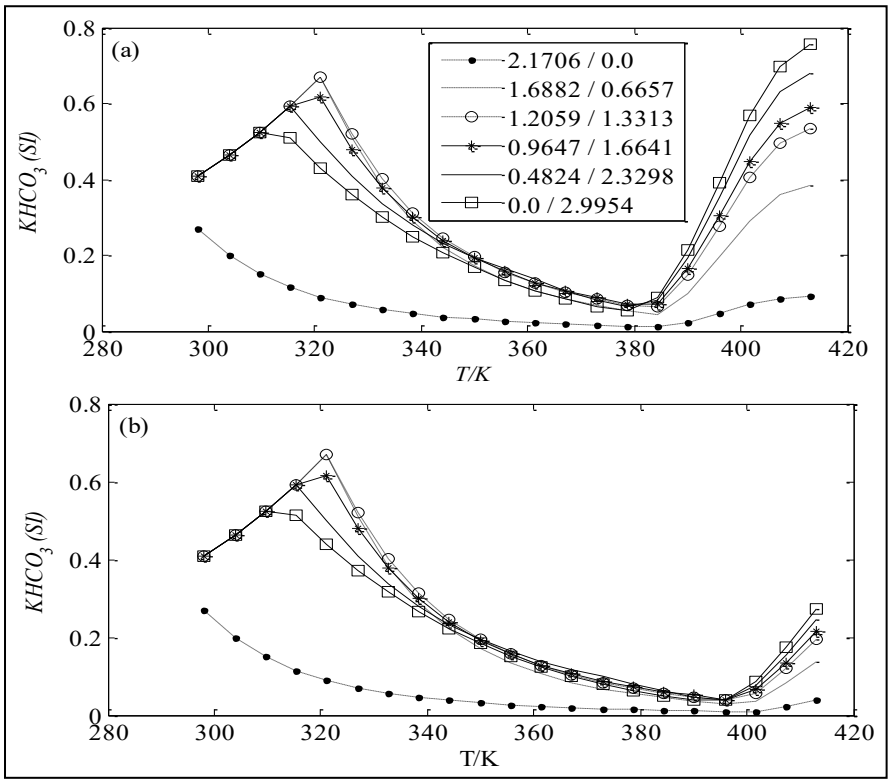

Figure 6. Effect of temperature and pressure on the bicarbonate solubility index for carbonate/bicarbonate mixture solution at pressures of 1 bar (a) and 2 bar (b).

List of symbols

T^{ref}	reference temperature, 298.15 K
T	current temperature
$\gamma_{\pm}$	mean activity coefficient
x	number of anions
y	number of cations
$\tau_{Ba,ca}$	$\tau_{aB} - \tau_{ca,B} + \tau_{B,ca}$
$\tau_{Bc,ac}$	$\tau_{cB} - \tau_{ca,B} + \tau_{B,ca}$
Xj	xj Cj (Cj=Zj for ions; Cj = unity for molecule)
B	solvent molecule
C	cation
A	anion
z_c	charge number of cation
z_a	charge number of anion
τ	binary energy interaction parameter
NC	number of the chemical species
$a_{(i,k,A,w)}$	Activity
A	Debjie Huckel parameter
N	mole number
W	Water
K	solubility product
K	stoichiometric coefficient for cation
A	degree of dissociation
ΔG^0	Gibbs energy at standard conditions
SI	solubility index
ρ	density
γ	activity coefficient
η	viscosity
m_1	molal concentration of K_2CO_3
m_2	molal concentration of $KHCO_3$

References

[1] A.L. Kohl, R. Nielsen, Gas Purification, 5th Ed., Gulf Publishing Co., Houston, 1997.

[2] K. Smith, U. Ghosh, A. Khan, M. Simioni, K. Endo, X. Zhao, S. Kentish, A. Qader, B. Hooper, G. Stevens, Energy Procedia 1 (2009) 1549-1555.

[3] M.R. Rahimpour, A. Z. Kashkooli, Chemical Engineering and Processing 43 (2004) 857-865.

[4] D. Wappel, A. Khan, D. Shallcross, S. Joswig, S. Kentish, G. Stevens, Energy Procedia 1 (2009) 125-131.

[5] F. Yi, H.K. Zou, G.W. Chu, L. Shao, J.F. Chen, Chemical Engineering Journal 145 (2009) 377–384.

[6] Benfield Process, http://www.uop.com (20.08.2010).

[7] G. Maxwell, Synthetic Nitrogen Products: A Practical Guide to the Products and Processes, Kluwer Academic, New York, 2004.

[8] K. Thomsen, Electrolyte Solutions: Thermodynamics, Crystallization, Separation methods, Lecture Notes, Technical University of Denmark, 2008.

[9] Foster Kofi Ayittey, Christine Ann Obek, Agus Saptoro, Kumar Perumal, Mee Kee Wong, Process modifications for a hot potassium carbonate-based CO2 capture system: a comparative study, greenhouse science and technology, volume 10, issue 1-2020

[10] C.C. Chen, Computer Simulation of Chemical Process with Electrolytes, Sc.D. Thesis, Massachusetts Institute of Technology, Cambridge, MA, USA, 1980.

[11] N. Liu, X. Zhao, Y. Wang, and W. Fei, Chinese Journal of Chemical Engineering, 18(2010) 538-543.

[12] M.D. Hilliard, Thermodynamics of Aqueous Piperazine/Potassium Carbonate/Carbon Dioxide Characterized by the Electrolyte NRTL Model within Aspen Plus, M.S. Thesis, The University of Texas at Austin, Austin, TX, 2005.

[13] A.H.G. Cents, D.W.F. Brilman, G.F. Versteeg, Chemical Engineering Science, 60(2005), 5830 – 5835.

[14] AspenTech, Physical Properties Data Reference Manual, Élan Computer Group, Inc., Mountain View, CA, USA, 1989.

[15] A. Haghtalab, V.G. Papangelakis and X. Zhu, Fluid Phase Equilibria, 220(2004) 199-209.

[16] J. Barthel, H. Krienke and W. Kunz, Physical Chemistry of Electrolyte Solutions, New York, 1998.

[17] R.G. Georgios, M. Kontogeorgis, Computer Aided Property Estimation for Process and Product Design: Computers Aided Chemical Engineering, 1st Ed., Elsevier 2004.

[18] R.D. Walker, A Study of Gas Solubilities and Transport Properties in Fuel Cell Electrolytes, Engineering and Industrial Experiment Station, MS Thesis, Gainesville, Florida, 1970.

[19] O.Eisa, M. Shuhaimi, Thermodynamic Study of Hot Potassium Carbonate Solution Using Aspen Pluus. World Academy of Science, Engineering and Technology (WASET), vol 4 2010-02-20.